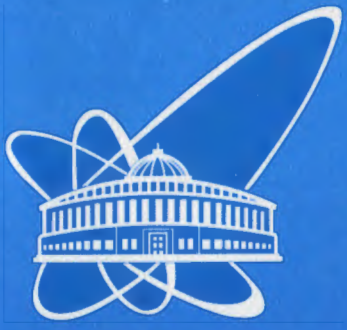

ОБЪЕДИНЕННЫЙ
ИНСТИТУТ
ЯДЕРНЫХ
ИССЛЕДОВАНИЙ

Дубна

E2-2002-117

G. N. Afanasiev[1], V. M. Shilov, Yu. P. Stepanovsky[2]

AMBIGUITIES IN THE OBSERVATION OF THE VAVILOV–CHERENKOV RADIATION

Submitted to «European Journal of Physics»

[1]E-mail: afanasev@thsun1.jinr.ru
[2]Institute of Physics and Technology, Kharkov, Ukraine

2002

1 Introduction

It is known that the frequency spectrum of a point-like charge moving uniformly with a velocity v greater than the light velocity in medium extends to infinity. The integral radiated energy and the photon number are infinite. This is due to the point-like structure of a moving charge whose infinite self-energy is a reservoir allowing charge to move uniformly despite the energy losses due to the radiation, ionization and the polarization of the surrounding medium. The easiest way of obtaining the finite frequency spectrum is to consider the charge of finite dimensions. This was done in a nice paper [1] where the charge density having zero dimensions in the transverse direction and the Gauss distribution along the motion axis was considered. The frequency spectrum obtained there, extended up to v/a, where a is the parameter of the Gauss distribution. Obviously, this charge distribution is rather unphysical. The next attempt was made in [2] where the charge distributions were chosen in the form of the spherical shell, Yukawa distribution and that of [1]. It should be noted that the authors of [1] and [2] related their charge densities to the laboratory frame. It seems to us that it is more natural to relate charge densities to the rest frame of the moving charge. There are two reasons for this. First, the charge form factor of a moving charge is the Fourier transform of a charge density related to the rest frame of a moving charge. Second, in another laboratory frame moving relative the initial one with a constant velocity, the charge density is no longer spherically symmetric. So, we prefer defining the charge density in its rest frame. Then, charge and current densities in the laboratory frame are obtained by the Lorentz transformation. Solving the Maxwell equations with these densities, we find electromagnetic field strengths and the radiated energy flux. This is essentially the procedure adopted by us. In addition to the current densities studied in [1,2], we considered the charge density uniformly distributed inside the sphere and the spherical Gauss distribution.

A charge uniformly moving in medium radiates if its velocity exceeds the light velocity in medium. If there is no external force supporting this motion, the charge should be decelerated. In the absence of dispersion, the total energy (obtained by the integration over the frequency spectrum) is infinite for the point-like charge. For the charge of finite dimensions, this quantity is finite. Equating it to the kinetic energy loss, one can find how moves a charge losing the energy due to the Cherenkov radiation. This is done in subsection (2.1).

Another way of getting the finite radiated energy is to take into account the medium dispersion. For the medium without damping, with dispersion law defined by a one-pole formula broadly used in optics, the finite expressions were obtained in [3] for the total (that is, integrated over ω) radiated energy and the number of photons. Equating the energy radiated per unit length to the kinetic energy loss we find how varies the charge velocity due to the Cherenkov radiation.

For the medium with damping, closed expessions for frequency distributions of the radiated energy and the number of photons were obtained in [3,4]. Yet, they were slightly inconvenient for applications, as they involved the Bessel functions

of complex argument. In this treatment, we use simple approximate radiation intensities found in [3], which, for the typical experimental conditions, agree with a great accuracy with the exact ones. They are applied to two substances for which the parametrization of dielectric permittivity is known. However, the following ambiguity arises. Due to the medium absorption, the position and the value of the frequency distribution on the surface of the observation cylinder essentially depend on the cylinde radius and the damping parameter. This means that, in the presence of damping, the Cherenkov frequency spectrum is not properly defined (since it depends on the observation distance).

So far, we implicitly assumed that the measuring device is in the same medium where the charge moves. However, the charge usually moves in one medium while observations are performed in another one. For example, in the initial Cherenkov experiments, the electrons moved in water, while the observations were made in air. Complications and ambiguities arising from such an experimental procedure are also discussed.

2 Cherenkov radiation from the charge of finite dimensions

Consider the charge of the finite dimensions moving uniformly in the medium with the velocity v directed along the z axis. Let its charge density in the reference frame where it is at rest, be spherically symmetric: $e\rho_{Ch}(r')$ where $r' = \sqrt{x'^2 + y'^2 + z'^2}$. In the laboratory frame (relative to which a charge moves with the velocity v), the charge and current densities are given by

$$\rho_L = e\gamma\rho_{Ch}(r), \quad j_z = v\rho_L,$$

where $r = [\rho^2 + \gamma^2(z - vt)^2]^{1/2}$, $\rho = \sqrt{x^2 + y^2}$, $\gamma = (1 - \beta^2)^{-1/2}$ and $\beta = v/c$. The Fourier transform of ρ_L is defined as

$$\rho_\omega = \frac{1}{2\pi} \int_{-\infty}^{\infty} dt \exp(i\omega t)\rho_L(t).$$

Making the change of variables ($t = z/v + \rho x/\gamma v$), we transform ρ_ω to the form

$$\rho_\omega = \frac{e}{\pi v} \exp(i\psi) f(\rho), \quad \psi = \omega z/v$$

where

$$f(\rho) = \rho \int_0^{\infty} \cos(\frac{\omega\rho}{\gamma v} x)\rho_{Ch}(\rho\sqrt{1 + x^2})dx.$$

The electric scalar and magnetic vector (only its z component differs from zero) potentials are

$$\Phi_\omega(x', y', z') = \frac{1}{\epsilon} \int \frac{1}{R} \exp(ik_n R)\rho_\omega(x', y', z')dV', \quad A_\omega = \beta\mu\epsilon\Phi_\omega.$$

Here $R = [(x-x')^2 + (y-y')^2 + (z-z')^2]^{1/2}$, $k_n = kn$, $k = \omega/c$, and $n = \sqrt{\epsilon\mu}$ is the refractive index of the medium with parameters ϵ and μ. Now we take into account the expansion

$$\frac{1}{R}\exp(ik_nR) = \sum_{m=0}^{\infty} \epsilon_m \cos m(\phi-\phi')\{i\int_{-k_n}^{k_n} dk_z \exp[ik_z(z-z')]G_m^{(1)} +$$

$$+\frac{2}{\pi}(\int_{-\infty}^{-k_n} + \int_{k_n}^{\infty})dk_z \exp[ik_z(z-z')]G_m^{(2)}\}, \qquad (2.1)$$

where

$$G_m^{(1)} = J_m(\sqrt{k_n^2 - k_z^2}\rho_<)H_m^{(1)})(\sqrt{k_n^2 - k_z^2}\rho_>),$$

$$G_m^{(2)} = I_m(\sqrt{k_z^2 - k_n^2}\rho_<)K_m(\sqrt{k_z^2 - k_n^2}\rho_>), \quad \epsilon_m = \frac{1}{1+\delta m,0}.$$

Further, J_m, $H_m^{(1)}$, I_m and K_m are the Bessel, Hankel, modified Bessel and Macdonald functions, resp. Substituting this expansion into Φ, and integrating over z' and ϕ', one gets

$$\Phi(x,y,z) = \frac{2\pi e}{\epsilon v}\exp(\frac{i\omega z}{v})[i\Theta(\beta_n - 1)H_0^{(1)}\Phi_1 + \frac{2}{\pi}\Theta(1-\beta_n)K_0\Phi_2], \quad A_z = \beta\epsilon\mu\Phi,$$

where

$$\Phi_1 = \int\int \rho^2 d\rho dt \cos(\frac{\omega\rho t}{\gamma v})J_0\rho_{Ch}(\rho\sqrt{1+t^2}),$$

and

$$\Phi_2 = \int\int \rho^2 d\rho dt \cos(\frac{\omega\rho t}{\gamma v})I_0\rho_{Ch}(\rho\sqrt{1+t^2}).$$

Here and further, we drop the arguments of the usual and modified Bessel functions if they are $k\rho\sqrt{n^2 - 1/\beta^2}$ and $k\rho\sqrt{1/\beta^2 - n^2}$, resp. The integration over ρ and t runs over the $(0,\infty)$ interval.

We intend to find the energy flux in the radial direction through the surface of a cylinder of the radius ρ coaxial with the motion axis. It coincides with the energy radiated per unit cylinder length and per unit frequency, and is given by

$$S_\rho = \frac{d^2\mathcal{E}}{dzd\omega} = -\pi\rho c(E_z H_\phi^* + E_z^* H_\phi).$$

Thus, we need E_z and H_ϕ. They are equal to

$$E_z = \frac{2\pi e i\mu\omega}{c^2}(1 - \frac{1}{\beta^2 n^2})\exp(\frac{i\omega z}{v})[i\Theta(\beta_n - 1)H_0^{(1)}\Phi_1 + \frac{2}{\pi}\Theta(1-\beta_n)K_0\Phi_2],$$

$$H_\phi = \frac{2\pi e}{c}\exp(\frac{i\omega z}{v})|k|\sqrt{|n^2 - 1/\beta^2|}[i\Theta(\beta_n - 1)H_1^{(1)}\Phi_1 + \frac{2}{\pi}\Theta(1-\beta_n)K_1\Phi_2].$$

Substituting them into S_ρ, one gets

$$S_\rho(\omega) = F \cdot S_{TF}, \tag{2.2}$$

where

$$S_{TF} = \frac{e^2\mu\omega}{c^2}(1 - \frac{1}{\beta^2 n^2}) \tag{2.3}$$

is the Tamm-Frank frequency distribution of the energy radiated by the uniformly moving point-like charge per unit length and per unit frequency [5], and

$$F = 16\pi^2\Phi_1^2 \tag{2.4}$$

is the factor taking into account the finite dimension of a charge (form factor, for short). The number of photons radiated by a moving charge per unit length of the cylindrical surface and per unit frequency is given by

$$N_\rho(\omega) = \frac{d^2N}{dzd\omega} = F \cdot N_{TF}, \tag{2.5}$$

where N_{TF} is the corresponding Tamm-Frank frequency distribution of the photon number

$$N_{TF} = \frac{\alpha\mu}{c}(1 - \frac{1}{\beta^2 n^2}), \tag{2.6}$$

and $\alpha = e^2/\hbar c$ is the fine structure constant.
The total energy and number of photons radiated per unit length of the cylindrical surface are obtained by integrating $S_\rho(\omega)$ and $N_\rho(\omega)$ over ω

$$S_\rho = \frac{d\mathcal{E}}{dz} = \int_0^\infty S_\rho(\omega)d\omega, \quad N_\rho = \frac{dN}{dz} = \int_0^\infty N_\rho(\omega)d\omega. \tag{2.7}$$

In what follows, when integrating (2.7), we assume the medium to be dispersion-free, that is, n does not depend on frequency. Consider particular cases.

1. Let the charge be uniformly distributed inside the sphere of the radius a:

$$\rho_{Ch}(r) = \rho_0\Theta(a - r), \quad \rho_0 = \frac{1}{(4\pi a^3/3)}. \tag{2.8}$$

Then,

$$\rho_L = e\gamma\rho_0\Theta\{a - [\rho^2 + \gamma^2(z - vt)^2]^{1/2}\}, \quad \rho_\omega = \frac{e\gamma\rho_0}{\pi\omega}\exp(\frac{i\omega z}{v})\sin(\frac{\omega}{\gamma v}\sqrt{a^2 - \rho^2}).$$

The form factor F entering into (2.2) is given by

$$F = \frac{9}{2}\pi\frac{J_{3/2}^2(y)}{y^3}, \tag{2.9}$$

where $y = ka\sqrt{n^2-1}$. The total radiated energy and the number of photons defined by (2.7) are given by

$$S_\rho = \frac{9\epsilon^2\mu}{4a^2}\frac{1-1/\beta^2n^2}{n^2-1}, \quad N_\rho = \frac{3\alpha\pi\mu}{5a}\frac{1-1/\beta^2n^2}{\sqrt{n^2-1}} \tag{2.10}$$

for $\beta > 1/n$ and zero otherwise.

2. The charge is distributed over the surface of the sphere

$$\rho(r) = \rho_0\delta(a-r), \quad \rho_0 = 1/(4\pi a^2). \tag{2.11}$$

The form factor F is

$$F = (\frac{\sin y}{y})^2, \quad y = ka\sqrt{n^2-1}. \tag{2.12}$$

The total energy

$$S_\rho = \int_0^\infty S_\rho(\omega)d\omega = \frac{\epsilon^2\mu(1-\beta^2n^2)}{a^2(n^2-1)}\int_0^\infty \frac{dy}{y}\sin^2 y \tag{2.13}$$

diverges while the total number of photons is finite:

$$N_\rho = \int_0^\infty N_\rho(\omega)d\omega = \frac{\alpha\mu\pi}{2a}\frac{1-1/\beta^2n^2}{\sqrt{n^2-1}}. \tag{2.14}$$

The divergence of S_ρ is due to the contribution of high frequencies. Formerly, frequency distribution $S_\rho(\omega)$ was obtained in [2] but with the form factor given by

$$F' = (\frac{\sin y'}{y'})^2, \quad \text{where} \quad y' = ka\sqrt{\epsilon}.$$

This leads to different physical predictions: for n slightly greater than 1, the form factor F also tends to 1 and the frequency distribution $S_\rho(\omega)$ tends to the Tamm-Frank one while the form factor F' and the frequency distribution $S_\rho(\omega)$, found in [2], are rapidly oscillating function of ω when $\epsilon \to 1$.

3. The charge is distributed according to the Gauss law

$$\rho_{Ch}(r) = \rho_0\exp(-\frac{r^2}{a^2}), \quad \rho_0 = 12/(\pi^{3/2}a^3). \tag{2.15}$$

Then,

$$\rho_\omega = \frac{e\gamma}{2\pi^2a^2v}\exp(i\psi)\exp(-\frac{\rho^2}{a^2})\exp(-\frac{k^2a^2}{4\beta^2}).$$

The form factor F is

$$F = \exp(-\frac{k^2a^2n^2}{2}). \tag{2.16}$$

The total radiated energy and the number of photons are finite now

$$S_\rho = \frac{e^2\mu}{a^2n^2}(1 - 1/\beta^2n^2), \quad N_\rho = \frac{\alpha\mu\pi^{3/2}}{an}(1 - 1/\beta^2n^2). \tag{2.17}$$

4. For the Yukawa charge distribution

$$\rho_{Ch}(r) = \rho_0\frac{\exp(-r/a)}{r}, \quad \rho_0 = \frac{1}{4\pi a^2}, \tag{2.18}$$

one gets

$$\Phi_1 = \frac{1}{4\pi}\frac{1}{1 + k^2a^2(n^2 - 1)}, \quad F = [\frac{1}{1 + k^2a^2(n^2 - 1)}]^2,$$
$$N_\rho(\omega) = N_{TF}F, \quad S_\rho(\omega) = S_{TF}F, \tag{2.19}$$

The integral number of emitted photons and the integral radiated energy are given by

$$N_\rho = \int d\omega N_\rho(\omega) = \frac{\pi\mu\alpha}{4a\sqrt{n^2 - 1}}(1 - \frac{1}{\beta^2n^2}),$$

$$S_\rho = \int d\omega S_\rho(\omega) = \frac{e^2\mu}{2a^2(n^2 - 1)}(1 - \frac{1}{\beta^2n^2}). \tag{2.20}$$

The following $S_\rho(\omega)$ was found in [2] for the Yukawa distribution

$$S_\rho = S_{TF}F, \quad \text{where} \quad F = \frac{1}{16\pi^2c^2(1 + k^2a^2\epsilon)}.$$

Obviously, this F is not reduced to 1 in the limit $a \to 0$ (as it should be). This is due to the extra factor $1/16\pi^2c^2$. The are two reasons why we cannot compare step by step our results with ones obtained in [1,2]. The first reason is a pure technical: the authors of [1,2] make the double Fourier transform over space and time variables, and then return to the frequency distribution using integration in k space. The advantage of our approach is that we always operate in a space-frequency representation, no intermediate steps are needed. The second reason is due to different definitions of charge densities. For example, we define the spherical charge density ρ_{Ch} in a moving system attached to a moving charge and then recalculate it into the laboratory frame using the Lorentz transformations, thus, obtaining ρ_L. On the other hand, authors of [2] postulate the spherical charge density ρ_{Ch} in the laboratory frame. It should be noted that, in the laboratory frame, the charge density due to the γ factors, cannot be spherically symmetrical (this is observed experimentally).

2.1 Cherenkov radiation as the origin of the charge deceleration

The following ambiguity arises. The Cherenkov radiation is usually associated with the radiation of a charge uniformly moving in medium. Since the moving charge

radiates, its kinetic energy should decrease. The energy radiated per unit length equals

$$\frac{d\mathcal{E}}{dz} = C(1 - 1/\beta^2 n^2) \tag{2.21}$$

for $\beta > 1/n$ and zero otherwise. The constant C, independent of β, is defined by one of Eqs. (2.10), (2.17) or (2.20). Obviously, (2.21) should be equal to the kinetic energy loss:

$$\frac{dT}{dz} = m_0 c^2 \frac{d}{dz} \frac{1}{\sqrt{1-\beta^2}} = -C(1 - 1/\beta^2 n^2). \tag{2.22}$$

Or, introducing the dimensionless variable $\tilde{z} = z/L, \quad L = m_0 c^2/C$, one gets

$$\frac{d}{d\tilde{z}} \frac{1}{\sqrt{1-\beta^2}} = -(1 - 1/\beta^2 n^2). \tag{2.23}$$

Integrating this equation, we get

$$(n^2-1)(\tilde{z} - \tilde{z}_0) = \frac{1}{2\alpha} \ln[(\frac{\alpha + \gamma^{-1}}{\alpha + \gamma_0^{-1}})^2 \cdot \frac{n^2\beta_0^2 - 1}{n^2\beta^2 - 1}] - n^2(\gamma - \gamma_0). \tag{2.24}$$

Here $\gamma = 1/\sqrt{1-\beta^2}, \gamma_0 = 1/\sqrt{1-\beta_0^2}, \quad \alpha = \sqrt{1 - 1/n^2}$, and β_0 is the charge velocity at the space point z_0. This equation, being resolved relative to β, defines the charge velocity $\beta(z)$ at a particular point of the motion axis. It follows from (2.24) that

$$\beta \to 1 - \frac{1}{2(1-1/n^2)^2 \tilde{z}^2}$$

for $\tilde{z} \to -\infty$ and

$$\beta \to \frac{1}{n}\{1 + \frac{1}{2}\exp[-2(n^2-1)\tilde{z}]\}$$

for $\tilde{z} \to \infty$. The dependence $\beta(\tilde{z})$ for typical parameters $n = 1.5, \beta_0 = 0.8$ and $z_0 = 0$ is shown in Fig. 1.

3 Cherenkov radiation in dispersive medium

Another way of obtaining the finite value of the radiated energy and the number of photons is to take into account the medium dispersion. We analyse two particular substances for which the parametrization of ϵ is known.

The first substance is iodine for which the parametrization of ϵ may be found in the Brillouin book [6]:

$$\epsilon = 1 + \frac{\omega_L^2}{\omega_0^2 - \omega^2 + ip\omega}. \tag{3.1}$$

Its resonance frequency lies in a far ultra-violet region and ϵ tends to 1 as $\omega \to \infty$. In this case, there is a critical velocity below and above of which the properties of

radiation differ appreciably. This parametrization is broadly used for the description of optical phenomena (see, e.g., [7,8]).

The following parametrization of ϵ:

$$\epsilon = \epsilon_\infty + \frac{\omega_L^2}{\omega_0^2 - \omega^2 + ip\omega} \tag{3.2}$$

with $p = 0$ was found in [9] for $ZnSe$. Its resonance frequency lies in a far infrared region and ϵ tends to the constant value when $\omega \to \infty$. There are two critical velocities for this case. The behaviour of radiation is essentially different above the large critical velocity, between smaller and larger critical velocities and below the smaller critical velocity. Despite the fact that parametrizations (3.1) and (3.2) are valid in a rather narrow frequency region, we apply them to the whole ω semi-axis. Since we will deal with frequency distributions of radiation, we can at any step limit consideration to the suitable frequency region.

The energy flux in the radial direction through the cylinder surface of the radius ρ is given by

$$\frac{d^3\mathcal{E}}{\rho d\phi dz dt} = -\frac{c}{4\pi} E_z(t) H_\phi(t).$$

Integrating this expression over the whole time of a charge motion and over the asimuthal angle ϕ, and multiplying it by ρ, one gets the energy radiated for the whole charge motion per unit length of the cylinder surface

$$\frac{d\mathcal{E}}{dz} = -\frac{c\rho}{2} \int E_z H_\phi dt.$$

Substituting here instead of E_z and H_ϕ their Fourier transforms and performing the time integration, one finds

$$\frac{d\mathcal{E}}{dz} = \int_0^\infty d\omega \sigma_\rho(\omega).$$

where

$$\sigma_\rho(\omega) = \frac{d^2\mathcal{E}}{dz d\omega} = -\pi\rho c E_z(\omega) H_\phi^*(\omega) + c.c.$$

is the energy radiated in the radial direction per unit frequency and per unit length of the observation cylinder. The identification of the energy flux with σ_ρ is typical in the Tamm-Frank theory [5] describing the unbounded charge motion in medium. Finding electromagnetic field strengths from the Maxwell equations, one gets

$$\sigma_\rho(\omega) = \frac{2ie^2\omega}{c^2}(1 - \frac{1}{\beta^2\epsilon}) x^* K_0(x)[K_1(x)]^* + c.c.. \tag{3.3}$$

Here $x = \sqrt{1 - \beta^2\epsilon} \cdot (\rho\omega/v)$. The sign of square root should be chosen in such a way as to guarantee the positivity of its real part. In this case, the modified Bessel functions decrease for $\rho \to \infty$. Equation (3.3), after reducing to the real form, was

used for the evaluation of radiation intensities in [3.4]. In the limit $p \to 0$, it passes into the Tamm-Frank formulae (2.3) and (2.6). For large $k\rho$ (k is the wave number, ρ is the radius of the observation cylinder C), the radiation intensity (3.3) goes into [3]

$$\sigma_\rho(\omega) = \frac{\epsilon^2\omega}{c^2}[(1 - \frac{\tilde{\epsilon}_r}{\beta^2})\sin\frac{\phi}{2} + \tilde{\epsilon}_i\cos\frac{\phi}{2}]\exp[-\frac{2\rho\omega}{v}(a^2+b^2)^{1/4}\cos\frac{\phi}{2}], \qquad (3.4)$$

where $\tilde{\epsilon}_r = \epsilon_r/(\epsilon_r^2+\epsilon_i^2)$, $\tilde{\epsilon}_i = -\epsilon_i/(\epsilon_r^2+\epsilon_i^2)$; ϵ_r and ϵ_i are real and imaginary parts of ϵ:

$$\epsilon = \epsilon_r + i\epsilon_i, \quad \epsilon_r = 1 + \frac{\omega_L^2(\omega_0^2-\omega^2)}{(\omega_0^2-\omega^2)^2+p^2\omega^2}, \quad \epsilon_i = -\frac{p\omega\omega_L^2}{(\omega_0^2-\omega^2)^2+p^2\omega^2}.$$

Further,

$$1-\beta^2\epsilon = a+ib, \quad a = 1-\beta^2\epsilon_r, \quad b = -\beta^2\epsilon_i,$$

$$\cos\frac{\phi}{2} = \frac{1}{\sqrt{2}}(1+\frac{a}{\sqrt{a^2+b^2}})^{1/2}, \quad \sin\frac{\phi}{2} = \frac{1}{\sqrt{2}}(1-\frac{a}{\sqrt{a^2+b^2}})^{1/2}. \qquad (3.5)$$

Usually, the condition $k\rho >> 1$ is fulfilled with great accuracy. For example, for the wavelength $\lambda = 4\cdot 10^{-5}$ cm and $\rho = 10$ cm, one gets $k\rho \approx 10^6$. Eq. (3.4) is valid for arbitrary dielectric permittivity. We apply it to (3.1) and (3.2).

3.1 Dielectric permittivity (3.1)

3.1.1 Dispersive medium without damping

For the sake of clarity, we consider at first $p = 0$. Then, from (3.3) one easily obtains the Tamm-Frank formulae (2.3) and (2.6). According to Tamm and Frank [5], the total radiated energy is obtained by integrating $\mathcal{E}_{TF}(\omega)$ over the frequency region satisfying $\beta n > 1$. It is easy to check that for $\beta > \beta_c = 1/\sqrt{1+\omega_L^2/\omega_0^2}$ this condition is satisfied for $0 < \omega < \omega_0$. For $\beta < \beta_c$ this condition is satisfied for $\omega_c < \omega < \omega_0$, where $\omega_c = \omega_0\sqrt{1-\beta^2\gamma^2/\beta_c^2\gamma_c^2}$. This frequency window narrows as β diminishes. For $\beta \to 0$, the frequency spectrum is concentrated near the ω_0 frequency. The total energy radiated per unit lentgh of the observation cylinder equals [3]

$$\frac{d\mathcal{E}}{dz} = \int_0^\infty S_\rho(\omega)d\omega = \frac{e^2\omega_0^2}{2c^2}[1 - 1/\beta^2 - \frac{1}{\beta^2\beta_c^2\gamma_c^2}\ln(1-\beta_c^2)] \qquad (3.6)$$

for $\beta > \beta_c$ and

$$\frac{d\mathcal{E}}{dz} = -\frac{e^2\omega_L^2}{2c^2}[1 + \frac{1}{\beta^2}\ln(1-\beta^2)] \qquad (3.7)$$

for $\beta < \beta_c$.

3.1.2 Energy balance due to the medium dispersion

According to Section 2, the influence of charge finite dimensions becomes essential for $ka \sim 1$. If for a we take $1fm$, then $\omega_f \sim 10^{23}s^{-1}$. On the other hand, in the presence of dispersion, the frequency spectrum of the radiation intensity extends up to ω_0. If we identify ω_0 with the ultraviolet frequency $\sim 10^{16}s^{-1}$, then, $\omega_0 << \omega_f$. This means that the influence of the dispersion begins at a much smaller frequency than the one due to the finite charge dimensions.

Since, in the presence of dispersion, $d\mathcal{E}/dz$ is finite (see (3.6) and (3.7)), one can extract $v(z)$ from the energy balance condition $dT/z = -d\mathcal{E}/dz$, similarly as it was done for the charge of finite dimensions. The following equations are valid now

$$\frac{d}{d\tilde{z}}\frac{1}{\sqrt{1-\beta^2}} = -(1 - \frac{1}{\beta^2\tilde{n}^2}) \tag{3.8}$$

for $\beta > \beta_c$ and

$$\frac{d}{d\tilde{z}}\frac{1}{\sqrt{1-\beta^2}} = (\frac{1}{\beta_c^2} - 1)[1 + \frac{1}{\beta^2}\ln(1-\beta^2)] \tag{3.9}$$

for $\beta < \beta_c$. Here we put

$$\tilde{n}^2 = [1 + (\frac{1}{\beta_c^2} - 1)\ln(1-\beta_c^2)]^{-1}, \quad \tilde{z} = \frac{z}{L}, \quad L = \frac{2m_0c^4}{e^2\omega_L^2}(\frac{1}{\beta_c^2} - 1).$$

Then, for $\beta > \beta_c$, one gets the following equation

$$(\tilde{n}^2 - 1)(\tilde{z} - \tilde{z}_0) = \frac{1}{2\alpha}\ln[(\frac{\alpha + \gamma^{-1}}{\alpha + \gamma_0^{-1}})^2 \cdot \frac{\tilde{n}^2\beta_0^2 - 1}{\tilde{n}^2\beta^2 - 1}] - \tilde{n}^2(\gamma - \gamma_0). \tag{3.10}$$

Here $\alpha = \sqrt{1 - 1/\tilde{n}^2}$; γ, γ_0 and z_0 are the same as in (2.24). It follows from (3.10) that

$$\beta \to 1 - \frac{1}{2(1 - 1/\tilde{n}^2)^2\tilde{z}^2}$$

for $\tilde{z} \to -\infty$. The velocity β_c is reached at

$$\tilde{z}_c = \tilde{z}_0 + \frac{1}{2\alpha((\tilde{n}^2 - 1)}\ln[(\frac{\alpha + \gamma^{-1}}{\alpha + \gamma_0^{-1}})^2 \cdot \frac{\tilde{n}^2\beta_0^2 - 1}{\tilde{n}^2\beta^2 - 1}] - \frac{\tilde{n}^2}{\tilde{n}^2 - 1}(\gamma - \gamma_0). \tag{3.11}$$

For $\beta > \beta_c$, the dependence $\beta(\tilde{z})$ extracted from (3.11) is shown in Fig.1 for typical parameters $\beta_c = 0.5$, $\beta_0 = 0.9$ and $\tilde{z}_0 = 0$. Below β_c, the asymptotic form of $\tilde{\beta}$ given by $\tilde{\beta} \sim \exp[-(\tilde{z} - \tilde{z}_c)/4\beta_c^2\gamma_c^2]$ and obtained from (3.9) is presented.

Although the energy balance is important from the theoretical viewpoint, it is slightly academic. The reason is that the energy losses due to the ionization of

medium atoms are much larger than the Cherenkov radiation losses. With a good accuracy, they are described by

$$dT/dz = -\frac{C}{\beta^2}F, \tag{3.12}$$

where C is a constant dependent on the medium properties and F is a function weakly dependent on β. For the electrons propagating in water $C \approx 1.65 Mev/cm$. On the other hand, the constant $e^2\omega_0^2/2c^2$ entering into (3.6) is $\sim 10^{-2} Mev/cm$ for $\omega_0 \approx 10^{16} s^{-1}$. Since $e^2\omega_0^2/2c^2 << C$, the ionization energy losses are much larger than the ones due to the Cherenkov radiation. This means that one may disregard the Cherenkov energy losses in (3.12). We can solve (3.12), if we put $F = 1$. Then,

$$\beta(z) = \frac{\sqrt{2}[x(x+4)]^{1/4}}{[\sqrt{x(x+4)} + x + 2]^{1/2}}. \tag{3.13}$$

Here $x = (z_f - z)/L$ and $L = m_0c^2/C$; z_f is the space point where $\beta = 0$. For $x \to 0$, $\beta \sim \sqrt{2}x^{1/4}$ and for $x \to \infty$, $\beta \sim 1 - 1/x^2$. The dependence $\beta(x)$ is shown in Fig. 2. The velocity β, as a function of z, drops almost instantly for small L. This justifies the validity of the Tamm problem [10] which involves a sudden transition from the charge uniform motion to the state of rest.

3.1.3 Dispersive medium with damping

Obviously, the nondamping behaviour of EMF is possible when the index of the exponent in (3.4) is small. This takes place, if $\cos\phi/2 \approx 0$. This, in turn, implies that $a = 1 - \beta^2\epsilon_r < 0$, and $b << |a|$. We need, therefore, the frequency regions where $1 - \beta^2\epsilon_r < 0$. Let $\beta_c < \beta < 1$, $\beta_c = 1/\sqrt{\epsilon_0}$, $\epsilon_0 = \epsilon(0) = 1 + \omega_L^2/\omega_0^2$. Then, $1 - \beta^2\epsilon_r < 0$ for $0 < \omega^2 < \omega_1^2$, where

$$\omega_{1,2}^2 = \omega_0^2 \pm \Omega_0 - \frac{1}{2}(p^2 + \beta^2\gamma^2\omega_L^2), \quad \Omega_0 = [\frac{1}{4}(p^2 + \beta^2\gamma^2\omega_L^2)^2 - \omega_0^2p^2]^{1/2}.$$

In particular, $\omega_1 = \omega_0$ for $\beta = 1$ and $\omega_1 = \sqrt{\omega_0^2 - p^2}$, $\omega_2 = 0$ for $\beta = \beta_c$.
Let $\beta_p^2 < \beta^2 < \beta_c^2$, where

$$\beta_p^2 = \frac{2p\omega_0 - p^2}{\omega_L^2 + 2p\omega_0 - p^2}$$

(it is therefore suggested that p is sufficiently small to guarantee the positivity of β_p^2. This is always fulfilled for transparent media where the Cherenkov radiation is observed). Then, $1 - \beta^2\epsilon_r < 0$ for $\omega_2 < \omega < \omega_1$. In particular, $\omega_1 = \omega_2 = \omega_0\sqrt{1 - p/\omega_0}$ for $\beta = \beta_p$. Finally, for $0 < \beta < \beta_p$ there is no room for $1 - \beta^2\epsilon_r < 0$.

We see that for $\beta > \beta_c$, the frequency distribution of the radiation differs from zero for $0 < \omega < \omega_1$, while for $\beta_p < \beta < \beta_c$ it is confined to the frequency window $\omega_2 < \omega < \omega_1$. Further decrease in β leads to the window narrowing. The window width disappears for $\beta = \beta_p$ when $\omega_1 = \omega_2 = \omega_0\sqrt{1 - p/\omega_0}$.

Now, the non-damping behaviour of EMF strengths in addition to $1 - \beta^2\epsilon_r < 0$ requires also $b << |a|$. This gives

$$\omega_L^2 \frac{\omega p - \omega_0^2 + \omega^2}{(\omega_0^2 - \omega^2)^2 + p^2\omega^2} << 1 - \frac{1}{\beta^2}$$

(it was taken into account that $1 - \beta^2\epsilon_r < 0$). Since the r.h.s. of this inequality is smaller than 0, its l.h.s. should also be smaller than 0. This takes place if

$$\omega < \sqrt{\omega_0^2 + p^2/4} - p/2.$$

For small damping this reduces to $\omega < \omega_0 - p/2$.

3.1.4 Application to iodine

As an example, we consider the dielectric medium with : $\epsilon_0 = 1 + \omega_L^2/\omega_0^2 \approx 2.24$. The parameters of this medium are close to those given by Brillouin ([6], p. 56) for iodine. As to ω_0, Brillouin recommends $\omega_0 \approx 4 \cdot 10^{16} s^{-1}$. This value of ω_0 is approximately 10 times larger than the average frequency of the visible region. However, since all formulae used for calculatons depend only on the ratios ω_L/ω_0 and p/ω_0, we prefer to fix ω_0 only at the final stage.

To illustrate analytic results obtained above, we present in Fig. 3 dimensionless spectral distributions $\sigma_p(\omega) = f(\omega)/(e^2\omega_0/c^2)$ for different charge velocities β and damping parameters p as a function of ω/ω_0. For $p = 0$ (Fig. 3 (a)), radiation intensities behave in the same way, as explained in section (3.1.1). The switching of the damping parameter p affects more strongly radiation intensities for $\beta < \beta_c$, than for $\beta > \beta_c$. For example, the radiation intensity corresponding to $\beta = 0.4 < \beta_c \approx 0.668$ is very small even for $p/\omega_0 = 10^{-8}$ (Fig. 3(b)). For larger p, the radiation intensity is so small, that it cannot be depicted in the scale used For instance, for $\beta = \beta_c$, the maximal value of the radiation intensity equals $2 \cdot 10^{-10}$ for $p/\omega_0 = 10^{-4}$ (Fig. 3(c)) and $3 \cdot 10^{-14}$ for $p = 10^{-2}$ (Fig. 3(d)). With the rising of p, the maximum of the frequency distribution shifts toward the smaller frequencies. This is due to the large value of the index under the sign of exponent in (3.4) (and, especially, to the large value of $\rho\omega/v$).

So far, we did not specify the resonance frequency ω_0. If, following Brillouin, we choose $\omega_0 = 4 \cdot 10^{16} sec^{-1}$ (which is approximately 10 times larger than average frequency of the visible light), then it follows from Fig. 3 (d) that for $p/\omega_0 = 10^{-2}$ (Brilloin recommends $p = 0.15$), frequency distributions are practically zero inside the region of the visible light corresponding to $\omega \approx \omega_0/10$. This means, in particular, that space-time distributions of the radiated energy corresponding to realistic p are formed mainly by photons lying in the far infra-red region and, therefore, there is no chance to observe them in the region of visible light.

Up to now, we considered the radiation intensities on the surface of the cylinder C of the radius $\rho = 10cm$. It is interesting to see how they look for smaller ρ. To

be concrete, consider the radiation intensities corresponding to $p/\omega_0 = 10^{-2}$. From Fig. 3 (d) we observe that the maximum of σ_ρ is at $\omega/\omega_0 = 2 \cdot 10^{-3}$ for $\beta = 1$ and $\rho = 10cm$. For $\rho = 1cm$ (Fig. 4 (a)), the maximum of the same radiation intensity is at $\omega/\omega_0 \approx 6 \cdot 10^{-3}$. This means that all frequency distributions shown in this figure are shifted towards the larger ω/ω_0. This tendency is supported by Figs. 4 (b-d) where the radiation intensities for $\rho = 10^{-2}cm$, $\rho = 10^{-4}cm$ and $\rho = 10^{-5}cm$ are presented.

3.2 Dielectric permittivity (3.2)

There is an important difference between parametrizations (3.1) and (3.2). It is seen that $\epsilon(\omega)$ given by (3.1) tends to unity for $\omega \to \infty$. This means that medium oscillators have no enough time to be excited in this limit. On the other hand, $\epsilon(\omega)$ given by (3.2) tends to ϵ_∞ in the same limit. This leads to the appearance of two critical velocities $\beta_\infty = 1/\sqrt{\epsilon_\infty}$ and $\beta_0 = 1/\sqrt{\epsilon_0}$, where $\epsilon_\infty = \epsilon(\omega = \infty)$ and $\epsilon_0 = \epsilon(\omega = 0) = \epsilon_\infty + \omega_L^2/\omega_0^2$. Now we evaluate the frequency distribution of the energy radiated by a point-like charge uniformly moving in ZnSe with the same parameters as in [9]. For the parametrizations (3.2) with $p = 0$, the radiation $(1 - \beta^2\epsilon < 0)$ condition is fulfilled in the following ω domains:

For the charge velocity greater than the larger critical velocity ($\beta > \beta_\infty$), the radiation condition $1 - \beta^2\epsilon < 0$ takes place if $0 < \omega < \omega_0$ and $\omega > \omega_1$. Here $\omega_1^2 = \omega_0^2(\beta^2\epsilon_0 - 1)/(\beta^2\epsilon_\infty - 1)$. At first glance it seems that for the parametrization (3.2) the frequency spectrum of the radiation extends to infinite frequencies. Fortunately, this is not so. According to section 2, the finite dimensions of a moving charge lead to the cut-off of the frequency spectrum approximately at $\omega_c = c/a$, where a is the charge dimension. If for a we take the classical electron radius (e^2/mc^2), then $\omega_c \sim 10^{23}sec^{-1}$, which is far above the frequency of the visible light ($\omega \sim 10^{15}sec^{-1}$). For $\beta \to \beta_\infty$, $\omega_1 \to \infty$, and only the low frequency part of the radiation spectrum survives. For the charge velocity between two critical velocities ($\beta_0 < \beta < \beta_\infty$), the radiation condition $1 - \beta^2\epsilon < 0$ takes place if $0 < \omega < \omega_0$. Finally, for the charge velocity smaller than the minor critical velocity ($0 < \beta < \beta_0$), the radiation condition $1 - \beta^2\epsilon < 0$ is realized in the frequency window $\omega_1 < \omega < \omega_0$. There is no radiation outside it. When $\beta \to 0$, $\omega_1 \to \omega_0$ and the frequency window becomes narrower.

3.2.1 Application to ZnSe

In Refs. [9], the following parameters of a dielectric permittivity (1.3) were found:

$$\epsilon_\infty = 5.79, \quad \epsilon_0 = 8.64, \quad \nu_0 = 6.3 \times 10^{12}Hz, \quad \omega_0 = 2\pi\nu_0 \approx 4 \cdot 10^{13}sec^{-1}.$$

The corresponding critical velocities are given by $\beta_\infty = 0.416$ and $\beta_0 = 0.34$.
For $\beta > \beta_\infty$, the frequency distribution is confined to the following ω regions: $0 < \omega < \omega_0$ and $\omega > \omega_1$. At $p = 0$, the radiation intensities behave in accordance with these predictions (Fig. 5). Let $p \neq 0$. For $\beta > \beta_\infty$, radiation intensities

corresponding to the high frequency branch ($\omega > \omega_1$) vary rather slowly with the rising of p (Figs. 6(a) and 7 (a)). On the other hand, the low energy branch of radiation intensity ($0 < \omega < \omega_0$) is more sensitive to the damping increase : it is practically invisible even for a rather small value of $p/\omega_0 = 10^{-6}$ (Fig. 7(a)). Let $\beta_0 < \beta < \beta_\infty$. At $p/\omega_0 = 10^{-8}$ and $p/\omega_0 = 10^{-6}$, the maximal values of radiation intensities are, respectively, four and forty times smaller than for $p = 0$ (Figs. 6(b) and 7 (b)). In addition, they are shifted towards the smaller ω. Still more rapidly decrease radiation intensities with rising p for $\beta < \beta_0$. For example, for $\beta = 0.2$ and $p/\omega_0 = 10^{-6}$, the maximal value of the radiation intensity is $\approx 5 \cdot 10^{-6}$.

The main result of this section is that, in absorbing media, both the value and position of the frequency distribution maximum crucially depend on the distance where observations are made. The diminishing of the radiation intensity is physically clear since only part of the radiated energy flux reaches observer if $p \neq 0$. Does the frequency shift of the radiation intensity maximum mean that any discussion on the frequency distribution of the radiation intensity should be supplemented by the indication of the observation distance? In the absence of absorption ($p = 0$), the index of the exponent in (3.4) is zero and the dependence on the cylindrical radius ρ drops out. At first glance, it is possible to associate the ρ independent frequency distribution of the radiation intensity with the pre-exponential factor in (3.4) which is the $\rho = 0$ limit of (3.4). But (3.4) is not valid at small distances. Instead, the exact Eq. (3.3) should be used there which is infinite at $\rho = 0$ (since a charge moves along the z axis).

4 Radiation of a charge moving in a cylindrical dielectric sample

Up no now we implicitly suggested that the radiation intensity is observed in the same medium where the charge moves. However, a charge usually moves in one medium (water, glass) while the observations are made in another medium (air, vacuum) (see, e.g., the nice Cherenkov review [11]). We intend now to consider arising complications. Consider a cylindrical sample C of the radius a filled with medium with the parameters ϵ_1 and μ_1. This sample is surrounded by another medium with parameters ϵ_2 and μ_2 such that $n_2 < n_1$. Let a charge move with a constant velocity v along the axis of C with a constant velocity v satisfying the inequality $1/n_1 < \beta < 1/n_2$ (that is, medium inside C is optically more dense than outside it). Formerly, this problem was considered by Frank and Ginzburg [12], who having written the general solution for arbitrary n_1 and n_2, applied it to a concrete case when the medium inside C was vacuum, while outside C was medium with the refractive index n_2. They obtained a remarkable result that despite the absence of the energy flux inside C, it reappears outside C if $\beta n_2 > 1$.

As to other possibilities, they remark that "Similarly, as it was done above, one

may easily consider other particular cases ($\beta n_1 > 1, \beta n_2 < 1; \beta n_1 > 1, \beta n_2 > 1$), which will not be considered here. We note only, that for $\beta n_2 < 1$, there are no radiation energy losses for both $\beta n_1 < 1$ and $\beta n_1 > 1$".
We consider in some detail the case corresponding to $n_2 < n_1, \beta n_1 > 1, \beta n_2 < 1$. One easily finds that the electromagnetic field arising from an unbounded charge motion along the axis of C equals

$$A_z = C_2\mu_2 \exp(i\psi)K_0(2), \quad H_\phi = C_2 k \exp(i\psi)\sqrt{1/\beta_2^2 - 1}K_1(2),$$

$$E_z = -ikC_2\mu_1(1/\beta_2^2 - 1)\exp(i\psi)K_0(2), \quad E_\rho = H_\phi/\beta\epsilon_2 \tag{4.1}$$

outside, C and

$$A_z = \mu_1 \exp(i\psi)[\frac{ie}{2c}H_0^{(1)}(1) + C_1 J_0(1)],$$

$$H_\phi = \exp(i\psi)kn_1\sqrt{1 - 1/\beta_1^2}[\frac{ie}{2c}H_1^{(1)}(1) + C_1 J_1(1)],$$

$$E_z = ik\mu_1 \exp(i\psi)(1 - 1/\beta_1^2)[\frac{ie}{2c}H_0^{(1)}(1) + C_1 J_0(1)], \qquad E_\rho = H_\phi/\beta\epsilon_1 \tag{4.2}$$

inside it. Here $\psi = kz/\beta, \beta_1 = \beta n_1, \beta_2 = \beta n_2$. The arguments of the Bessel functions are $2 = k\rho\sqrt{1/\beta^2 - n_2^2}$ for $\rho > a$ and $1 = k\rho\sqrt{n_1^2 - 1/\beta^2}$ for $\rho < a$.The coefficients C_1 and C_2 are found from the continuity of H_ϕ and E_z at $\rho = a$:

$$C_1 = \frac{e}{2c}[\frac{1}{\triangle}(n_1\mu_2\sqrt{1/\beta_2^2 - 1}K_0N_1 + n_2\mu_1\sqrt{1 - 1/\beta_1^2}K_1N_0) - i], \tag{4.3}$$

$$C_2 = \frac{e\mu_1}{\pi cka\triangle}\sqrt{\frac{1 - 1/\beta_1^2}{1/\beta_2^2 - 1}}, \quad \triangle = n_1\mu_2\sqrt{1/\beta_2^2 - 1}K_0J_1 + \mu_1 n_2\sqrt{1 - 1/\beta_1^2}K_1J_0.$$

The arguments of the usual and modified Bessel functions entering into (4.3) are $kan_1\sqrt{1 - 1/\beta_1^2}$ and $kan_2\sqrt{1/\beta_2^2 - 1}$, respectively. We evaluate now the energy fluxes.

4.1 Radial energy flux

The radial energy flux is

$$\sigma_\rho = \frac{d^2\mathcal{E}}{dzd\omega} = -\pi\rho c(E_z H_\phi^* + c.c.). \tag{4.4}$$

Obviously, it equals zero outside C and

$$\sigma_\rho = -\pi\rho c k^2 \mu_1 n_1 (1 - 1/\beta_1^2)^{3/2}[(-\frac{e}{2c}H_0^{(1)} + iC_1J_0)(-\frac{ie}{2c}H_1^{(2)} + C_1^*J_1) +$$

$$+(-\frac{e}{2c}H_0^{(2)} - iC_1^*J_0)(\frac{ie}{2c}H_1^{(1)} + C_1J_1)] = 0$$

inside C (it was taken into account that $ImC_1 = -e/2c$). Thus, the radial energy flux equals zero inside C too. This is due to the fact that the contribution of the terms with the product of Hankel functions in the energy flux is compensated by the terms with the product of Bessel and Hankel functions. The following complication arises. Let the detector be placed outside C, that is, in medium where $\beta n_2 < 1$. In fact, this is a typical sitution in Cherenkov experiments. For example, in classical Cherenkov experiments [11], the electrons moved in a vessel filled with water, while the observations of the Cherenkov light were made in air , in a dark room, by a human eye. There is no radial energy flux outside C. Then, how the Cherenkov radiation can be observed there? One may argue that since the human eye is filled with the substance having the refractive index approximately equal to that of water, the Cherenkov radiation reappears in it (similarly to the appearance of the radiation in the medium surrounding the vacuum channel with a charge moving along its axis [12]) and, therefore, it could be detected. However, now there are known substances with large refractive indices. Does this mean that the radial energy flux cannot be detected outside C (for this, it is enough to use the collimator selecting only the photons emitted in the radial direction) if the measuring device is fabricated from the substance with the refractive index n_2 smaller than $1/\beta$ and n_1 ? The possible answer gives the following section where the energy flux in the direction parallel to the motion axis will be evaluated.

4.2 Energy flux along the motion axis

The energy flux parallel to the motion axis is

$$\sigma_z = \frac{d^2\mathcal{E}}{d\rho d\omega} = \pi\rho c(E_\rho H_\phi^* + c.c.). \tag{4.5}$$

It equals

$$\sigma_z = \frac{\rho e^2\mu_1^2\mu_2(1-1/\beta_1^2)}{\pi v a^2 \triangle^2}[K_1(k\rho n_2\sqrt{1/\beta^2-1})]^2 \tag{4.6}$$

outside C and

$$\sigma_z = \pi\rho c\mu_1 k^2(1-1/\beta_1^2)[\frac{e^2}{4c^2}(J_1^2+N_1^2) + J_1^2|C_1|^2 - \frac{e}{c}(N_1C_{1r} - J_1C_{1i})], \tag{4.7}$$

inside it. Here C_{1r} and C_{1i} are the real and imaginary parts of D:

$$C_{1r} = \frac{e}{2c}\frac{1}{\triangle}(n_1\mu_2\sqrt{1/\beta_2^2-1}K_0N_1 + n_2\mu_1\sqrt{1-1/\beta_1^2}K_1N_0), \quad C_{1i} = -\frac{e}{2c}.$$

In general, σ_z is exponentially small outside C, except for ω satisfying $\triangle = 0$. For these ω, σ_z is infinite. For large ka, equation $\triangle = 0$ is reduced to

$$kan_1\sqrt{\beta_1^2-1} = \frac{\pi}{4} - \arctan\frac{\epsilon_2\sqrt{\beta_1^2-1}}{\epsilon_1\sqrt{1-\beta_2^2}} + m\pi, \tag{4.8}$$

where m is integer. The distance between the neighbouring maxima of σ_z is $\Delta\omega = \pi c/(a n_1 \sqrt{\beta_1^2 - 1})$. For the cylinder radius $a \sim 10cm$, the $\Delta\omega$ is about $10^{10} s^{-1}$. The typical optical frequency is about $5 \cdot 10^{15} s^{-1}$. Since the real Cherenkov detector has the finite frequency resolution width (several $10^{15} s^{-1}$ units) it inevitably covers many maxima of σ_z and, therefore, the measuring device oriented parallel to the motion direction will detect the almost continuous radiation.

5 Optical interpretation

A charge uniformly moving inside the dielectric cylinder C emits the light ray at the Cherenkov angle θ_1 ($\cos\theta_1 = 1/\beta n_1$) towards the charge motion axis. Let this ray intersect the cylinder surface at some point and let i be the incidence angle (Fig. 8). It is easy to check that $\sin i = \cos\theta_1$. According to classical optics (see, e.g., [7,8]), the incidence i, reflected i' and refractive r angles are interrelated as follows: $i = i'$, $\sin r = (n_1/n_2)\sin i$. It follows from Fig.8 that $\sin r = \cos\theta_2$, where θ_2 is the inclination angle of the light ray moving in medium 2 towards the z axis. Therefore, $\cos\theta_2 = (n_1/n_2)\cos\theta_1 = 1/\beta n_2$. That is, if $\beta n_2 > 1$, the light ray in medium 2 propagates at the angle θ_2 towards the motion axis. Otherwise ($\beta n_2 < 1$), the total internal reflection takes place. Due to the translational symmetry of the problem, the same total internal reflection takes place in all other points where a given light ray meets the cylinder surface. This means that the light ray emitted by a moving charge remains within the infinite cylindrical sample if $\beta n_2 < 1$.

The situation slightly changes if the cylindrical sample has a finite length. In order not to deal with the transition radiation (arising when the moving charge passes through the boundaries of mediums 1 and 2), we consider the charge motion completely confined within C (Fig. 9). This situation was realized in the original Cherenkov experiments where Compton electrons were completely absorbed in water. Usually, this situation is described in terms of the so-called Tamm problem [10], where the charge moves uniformly with the velocity $\beta > n_1$ on a finite space interval. After a number of reflections at the surface of C, a particular light ray reaches the bottom of a cylindrical sample. It is easy to check that its incidence angle coincides with θ_1. The refractive angle is given by

$$\sin r' = \frac{n_1}{n_2}\sin\theta_1 = \frac{n_1}{n_2}\sqrt{1 - \frac{1}{\beta^2 n_1^2}}.$$

Obviously, the light ray leaves C through its bottom if $\sin r' < 1$. This is equivalent to

$$\beta < min(\frac{1}{n_2}, \frac{1}{\sqrt{n_1^2 - n_2^2}}).$$

It follows from this that if $n_2 > n_1/\sqrt{2}$, then the light ray passes through the bottom of C and propagates in medium 2 at the angle $\theta_2' = r'$ towards the motion axis. Let

$n_2 < n_1/\sqrt{2}$. Then, for $\beta < 1/\sqrt{n_1^2 - n_2^2}$, the light ray propagates in medium 2 at the same angle θ_2' towards the motion axis. On the other hand, for

$$\frac{1}{\sqrt{n_1^2 - n_2^2}} < \beta < \frac{1}{n_2},$$

the total internal reflection takes place on the bottom of C as well. Therefore, in this case the light ray emitted by a moving charge remains within C.

Consider the dielectric sphere S of the radius R filled by the substance with refractive index n_1 and surrounded by the substance with refractive index n_2 (Fig. 10). Let a charge move uniformly in the space interval $(-z_0, z_0)$ lying completely inside S and let its velocity be such that $1/n_1 < \beta < 1/n_2$. Elementary calculations show that the Cherenkov γ ray emitted at the point z of the motion axis, outside S propagates under the angle

$$\theta_2 = \theta + \arcsin[\frac{n_1}{n_2}\sin(\theta_1 - \theta)] \tag{5.1}$$

towards the motion axis. Here θ_1 is defined by $\cos\theta_1 = 1/\beta_1 n$ and θ is related to the charge particular position z as follows

$$\cos\theta = \frac{z}{R}\sin\theta_1 + \cos\theta_1\sqrt{1 - \frac{z^2}{R^2}\sin^2\theta_1}.$$

Obviously, $\cos\theta$ changes in the interval

$$-\frac{z_0}{R}\sin\theta_1 + \cos\theta_1\sqrt{1 - \frac{z_0^2}{R^2}\sin^2\theta_1} < \cos\theta < \frac{z_0}{R}\sin\theta_1 + \cos\theta_1\sqrt{1 - \frac{z_0^2}{R^2}\sin^2\theta_1}$$

when a charge moves from $z = -z_0$ to $z = z_0$. Substituting this into (5.1), we find the angular interval, where the Cherenkov radiation differs from zero outside S.

This means that the Cherenkov radiation has more chances to leave the sphere than the cylinder. The reason is that the Cherenkov γ ray meets the sphere surface at different incidence angles depending on the charge position on the motion axis.

The semi-intuitive consideration of this section:
i) shows that the observation of the Cherenkov radiation strongly depends on the boundaries surrounding the volume where a charge moves;
ii) defines conditions under which the Cherenkov radiation can penetrate from the medium 1 with $\beta n_1 > 1$ into the medium 2 with $\beta n_2 < 1$ without exhibiting the total internal reflection on their boundary. However, only concrete calculations can determine the value of the radiation intensity in the nedium 2.

6 Discussion

Sections 3-5 rise uneasy questions concerning the observation of the Cherenkov radiation for the unbounded and bounded charge motions.

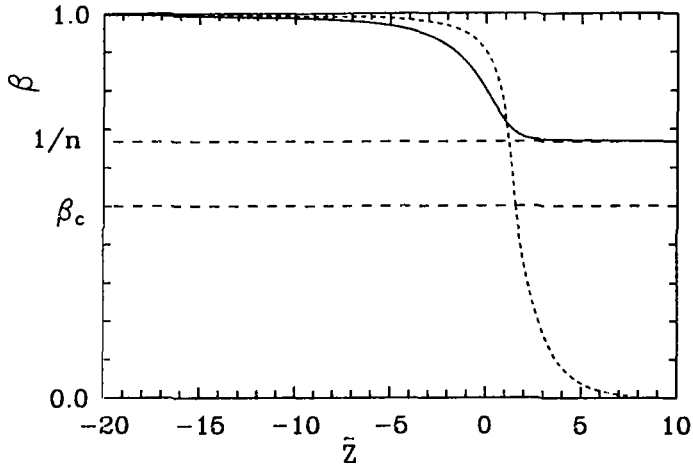

Figure 1: This figure shows how a moving charge is decelerated when all its energy losses are due to the Cherenkov radiation. The solid curve corresponds to the charge of finite dimensions moving in dispersion-free medium. The charge velocity approaches $1/n$ for $\tilde{z} \to \infty$. The pointed curve corresponds to the point-like charge moving in dispersive medium. Its velocity equals β_c at $\tilde{z} = \tilde{z}_c$. Below β_c, the asymptotic form of β given by $\beta \sim \beta_c \exp[-(\tilde{z} - \tilde{z}_c)/4\beta_c^2\gamma_c^2]$ was used.

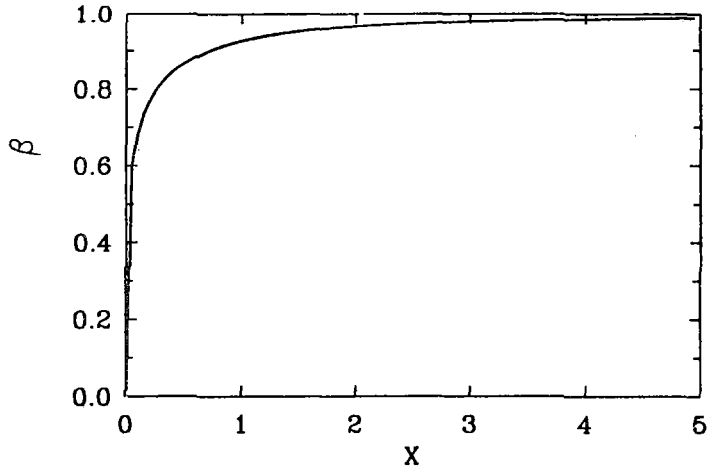

Figure 2: This figure shows how a charge is decelerated due to the ionization energy losses described by (3.8). Here $x = (z_f - z)/L$, z_f is the space point where $\beta = 0$ and L is the same as in (3.10).

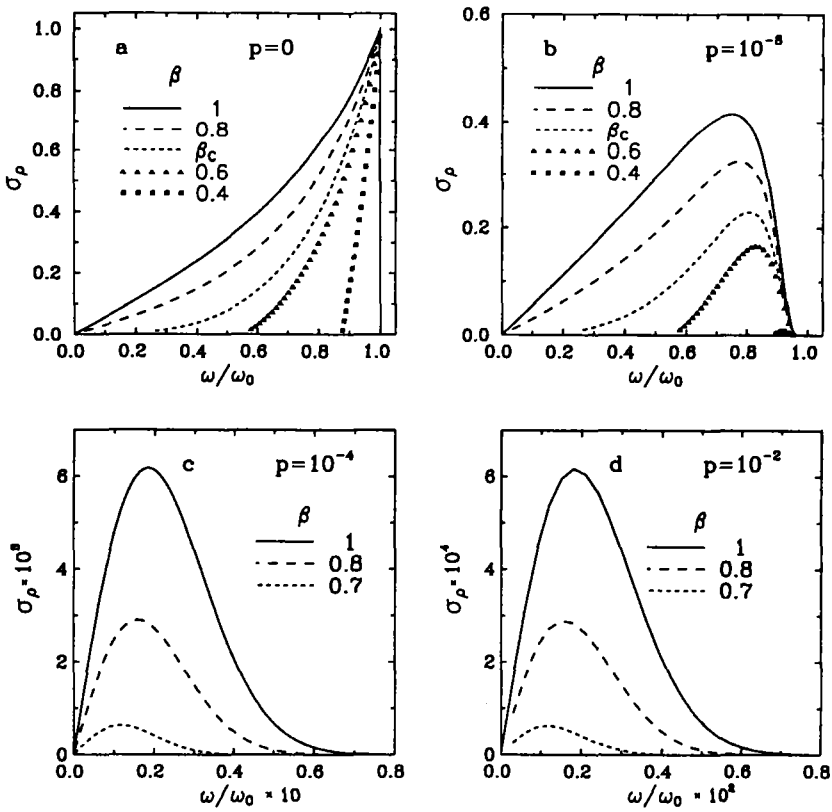

Figure 3: Radiation intensities corresponding to dielectric permittivity (3.1) for a number of velocities and damping parameters p (in ω_0 units). The radius of the observation cylinder $\rho = 10cm$. Other medium parameters are the same as suggested by Brilluoin for iodine. It is seen that the radiation spectrum shifts towards low frequencies with the rising of p.

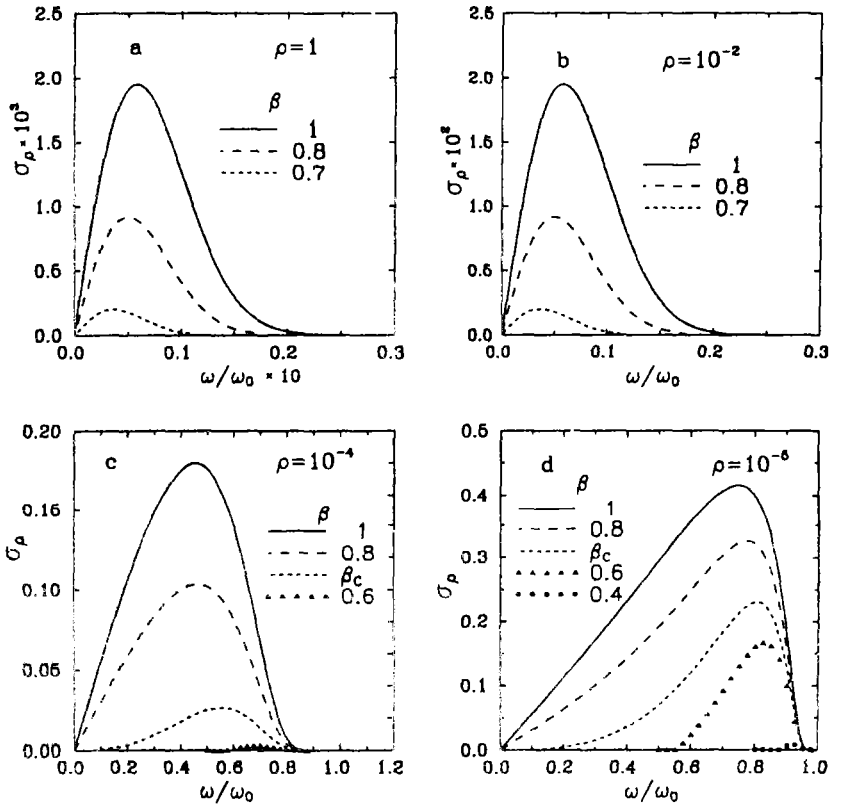

Figure 4: Radiation intensities corresponding to dielectric permittivity (3.1) for $p/\omega_0 = 10^{-2}$ and for a number of velocities and observation cylinder radii ρ (in cm). It is seen that the frequency distribution of the radiation crucially depends on the radius ρ. This leads to the ambiguity in interpretation of experimental data. The ρ dependence of the frequency spectrum disappears in the absence of damping.

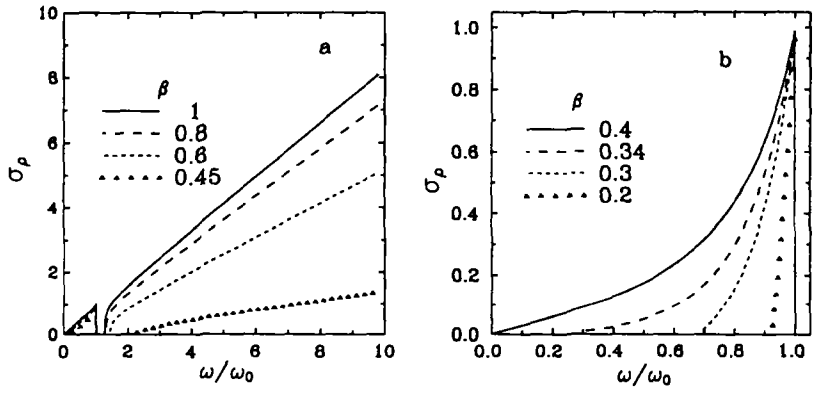

Figure 5: Radiation intensities corresponding to dielectric permittivity (3.2) for $p = 0$ and a number of a charge velocities. The medium parameters are the same as for $ZnSE$. There are two critical velocities: $\beta_\infty \approx 0.416$ and $\beta_0 \approx 0.34$. For $\beta > \beta_\infty$, there are two frequency regions ($0 < \omega < \omega_0$ and $\omega_1 < \omega < \infty$) to which frequency distributions are confined (a). When $\beta \to \beta_\infty, \omega_1 \to \infty$. For $\beta_0 < \beta < \beta_\infty$, the radiation is confined to the frequency region $0 < \omega < \omega_0$ ((b), $\beta = 0.4$ and 0.34). For $0 < \beta < \beta_0$, the radiation is confined to the frequency region $\omega_1 < \omega < \omega_0$. When $\beta \to 0, \omega_1 \to \omega_0$ and the frequency window becomes narrower ((b), $\beta = 0.3$ and 0.2).

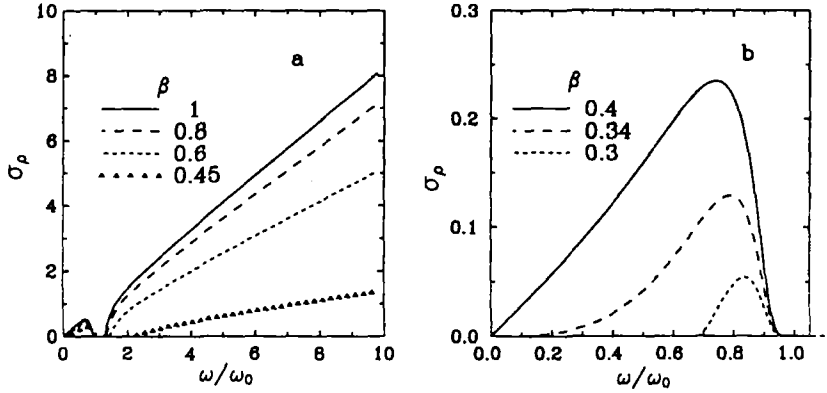

Figure 6: The same as in Fig.5, but for the nonzero damping parameter $p/\omega_0 = 10^{-8}$. It is seen that for $\beta > \beta_\infty$ (a), the high-frequency branch of spectrum is almost the same as in the absence of damping. Radiation intensities in the low-frequency part of the spectrum are two times smaller than for $p = 0$. For $\beta < \beta_\infty$ (b), the frequency spectrum is more sensitive to the change of p. Its position is shifted towards the smaller ω. For $\beta < \beta_0$, the radiation intensities are very small. For example, for $\beta = 0.2$, the maximal value of the radiation intensity is $\approx 5 \cdot 10^{-6}$. The cylinder radius $\rho = 10cm$

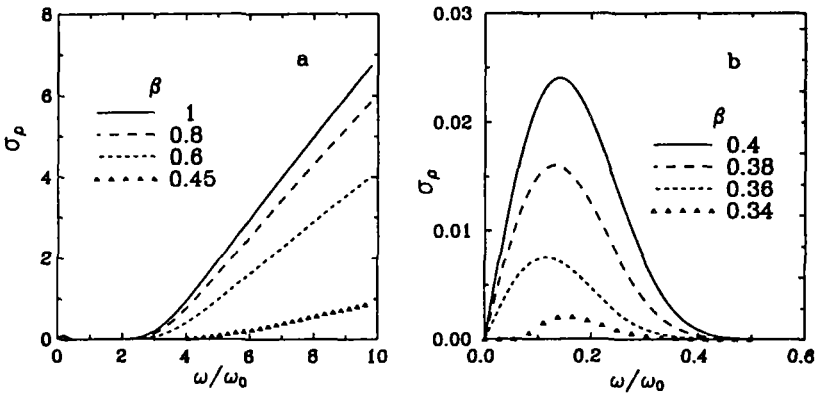

Figure 7: The same as in Fig.6, but for the larger $p/\omega_0 = 10^{-6}$. For $\beta > \beta_\infty$, the low-frequency part of the spectrum practically disappears (a). For $\beta_0 < \beta < \beta_\infty$ (b), the frequency spectrum is shifted towards the smaller ω and the radiation intensities are approximately ten times smaller than those in Fig. 6. The radiation intensity corresponding to $\beta = \beta_0 = 0.34$ is multiplied by 100 (that is, the shown curve should be decreased in 100 times). For $\beta < \beta_0$ the radiation intensities are small and cannot be presented in this scale. The cylinder radius $\rho = 10cm$. Comparing this figure with Figs. 5 and 6, we observe that the position of the frequency spectrum maximum crucially depends on the damping parameter.

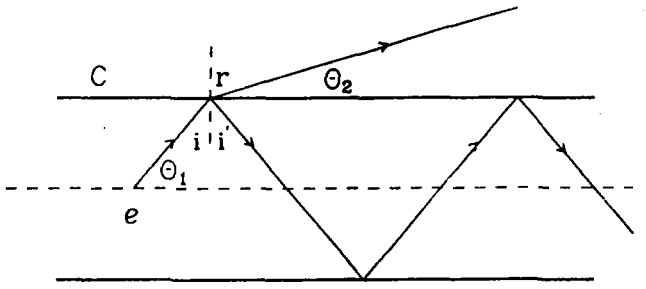

Figure 8: The infinite cylindrical dielectric sample C with refractive index n_1 surrounded by the medium with refractive index n_2. A charge moving in C, emits γ ray at the Cherenkov angle θ_1. This γ ray leaves C if $\beta n_2 > 1$. Otherwise, it exhibits the total internal reflection and remains within C.

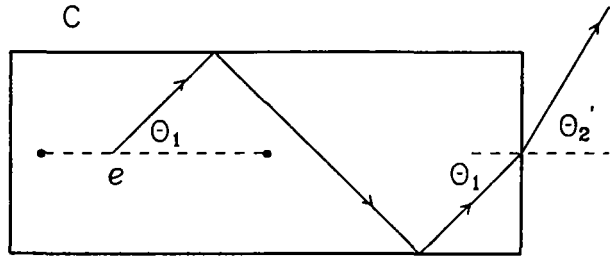

Figure 9: A charge moves in a finite dielectric sample C. There are additional possibilities for the Cherenkov γ ray to leave C through its bottom (see the text).

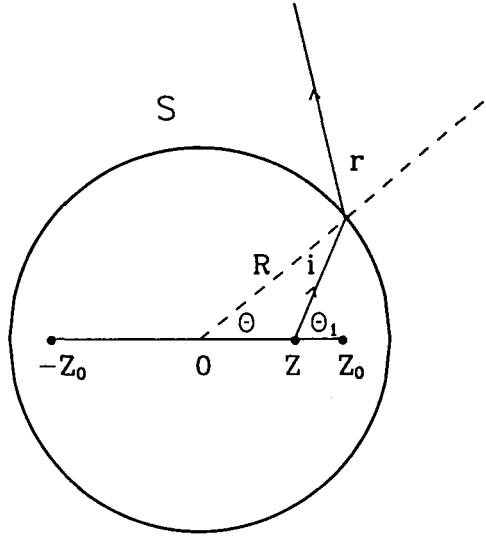

Figure 10: There are more chances for the Cherenkov γ ray emitted by a moving charge to leave the sphere S, than the dielectric cylinder C. The reason is that the Cherenkov γ ray meets S under different incidence angles depending on the charge position z in the motion interval $(-z_0, z_0)$. Here i and r are the incidence and refractive angles, resp.

In fact, it was shown in section 3 that for the charge moving in an absorptive medium not only the value of the maximum of the radiation frequency distribution (this is not surprising), but its position as well, crucially depend on the observation distance and damping parameter. Does this mean that experimentalists should indicate the observation distance when presenting measured frequency distributions of the radiated energy?.

In section 4, the complication was discussed arising when a charge moves in medium 1 for which the Cherenkov radiation condition $\beta n_1 > 1$ is fulfilled, while measurements are made in another medium 2 with $\beta n_2 < 1$. If we associate the energy radiated by a charge moving in the medium 1 with the radial (in the cylindrical geometry) energy flux (this is a usual thing in the Tamm-Frank radiation theory), the theory tells us that the energy radiated into the medium 2 is zero. Then, how to interpret the results of experiments performed under the same conditions and in which the Cherenkov photons were detected?. On the other hand, if we associate the radiated energy with the energy flux in the direction parallel to the motion axis, the energy radiated into the medium 2 is exponentially small for all frequencies except for the infinite set of discrete frequencies. Probably, the radiation observed in Cherenkov-like experiments with cylindrical geometry is due to this energy flux. The distance between the neighbouring representatives of this set is so small than the discrete nature of the frequency spectrum could hardly be resolved experimentally.

A precaution is needed. Sometimes, experimentalists (see, e.g., [13,14]) install inside the cylindrical volume C (especially, when it is filled with a gas) a mirror inclined under the angle $\pi/4$ towards the motion axis, This mirror reflects the σ_z component (4.7) of the internal energy flux in the direction perpendicular to the motion axis, thus, making possible to observe the energy flux in the radial direction outside C.

Optical considerations presented in section 5 show that the above ambiguity partly disappears when a charge moves inside the dielectric sphere. Does this mean that the observation of the Cherenkov radiation crucially depend on the experimental installation geometry ?

7 Conclusion

We briefly summarize the main results obtained:

1. It is analysed how finite dimensions of a moving charge affect the frequency spectrum of the radiated energy. It is shown that the frequency spectrum extends up to ka, where k and a are the wave number and the typical dimension of a moving charge, respectively.

2. It is shown how a charge should move in medium if, in the absence of external force, all its energy losses were due to the Cherenkov radiation. The analytic formula is obtained for the charge moving in medium with ionization losses.

3. Frequency distributions of the energy radiated by a charge moving in medium are evaluated for two concrete substances for which the parametrizations of dielectric

permittivity are known. The difficulties associated with the definition of the radiated energy flux, when the measurements are made in absorptive medium, are discussed.

4. There are discussed complications arising when a charge moves in the medium where the Cherenkov radiation condition is fulfilled, while the observations of the radiated energy are made in another medium where this condition is not fulfilled.

References

[1] Smith G.E., 1993, Amer. J. Phys., 61, 147.

[2] Villaviciencio M., Roa-Neri J.A.E. and Jimenez J.L., 1996, Nuovo Cimento B, 111, 1041

[3] Afanasiev G.N. and Kartavenko V.G., 1998, J. Phys. D, 31, 2760.

[4] Afanasiev G.N., Kartavenko V.G. and Magar E.N., 1999, Physica B, 269, 95.

[5] Frank I.M., 1988, *Vavilov-Cherenkov Radiation*, (Moscow, Nauka), in Russian.

[6] Brillouin L., 1960, *Wave Propagation and Group Velocity*, (New York and London, Academic Press).

[7] Born M. and Wolf E., 1975, *Principles of Optics*, (Oxford, Pergamon).

[8] Landau L.D. and Lifshitz E.M, 1960, *Electrodynamics of Continuous Media*, (Oxford, Pergamon).

[9] Li H., 1984, Chem. Ref. Data, 13, 102; Gobel A. et al., 1999, Phys. Rev B 59, 2749; Hattori et al., 1973, Opt. Commun., 7, 229; Jensen B., Torabi A., 1983, Infrared Phys., 23, 359.

[10] Tamm I.E., 1939, J.Phys. USSR, 1, 439.

[11] Cherenkov P.A., 1944, Trudy FIAN, 2, No 4, p.3.

[12] Ginzburg V.L. and Frank I.M., 1947, Dokl. Acad. Nauk SSSR, 56, 609.

[13] Aitken D.K., Jennings R.E., Parsons A.S.L. and Walker R.N.F., 1963, Proc. Phys. Soc., 82, 710.

[14] Ruzicka J. and Zrelov V.P., 1993, Czech. J. Phys., 43, 551.

Received on May 17, 2002.